

## Supporting information:

# Multitechnique investigation of Dy<sub>3</sub> – Implications for Coupled Lanthanide Clusters

Maren Gysler, Fadi El Hallak, Liviu Ungur, Raphael Marx, Michael Hakl, Petr Neugebauer, Yvonne Reckkemmer, Yanhua Lan, Ilya Sheikin, Milan Orlita, Christopher E. Anson, Annie K. Powell, Roberta Sessoli, Liviu F. Chibotaru, Joris van Slageren

## Content

Crystal structure .....	2
Luminescence measurements:.....	3
MCD measurements:.....	4
Ab initio calculations .....	5
EPR investigations .....	8
FIR investigations.....	10
Torque investigations.....	11
Improvement of the model.....	13
Supplementary references.....	17

## Crystal structure

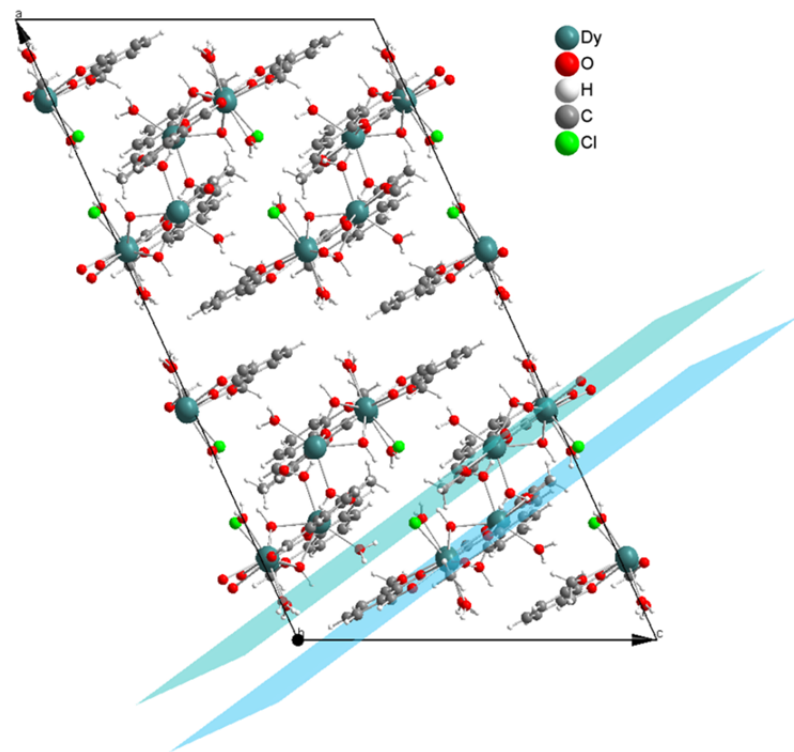


**Fig. S1.** Crystal structure of  $\text{Dy}_3$  as seen onto ac plane. The b axis goes into the plane of the paper. The two symmetry-related triangles are highlighted. They make an angle of  $5.2^\circ$  with each other.

## Luminescence measurements:

The luminescence spectra were recorded using a home built spectrometer using an excitation wavelength of  $\lambda_{ex} = 340$  nm. The excitation and emission slit widths were 5nm. Fig. S2 shows the spectra at 5K and room temperature for a powder sample on vacuum grease. Attempted direct excitations of ff transitions of Dy<sup>3+</sup> were been successful.

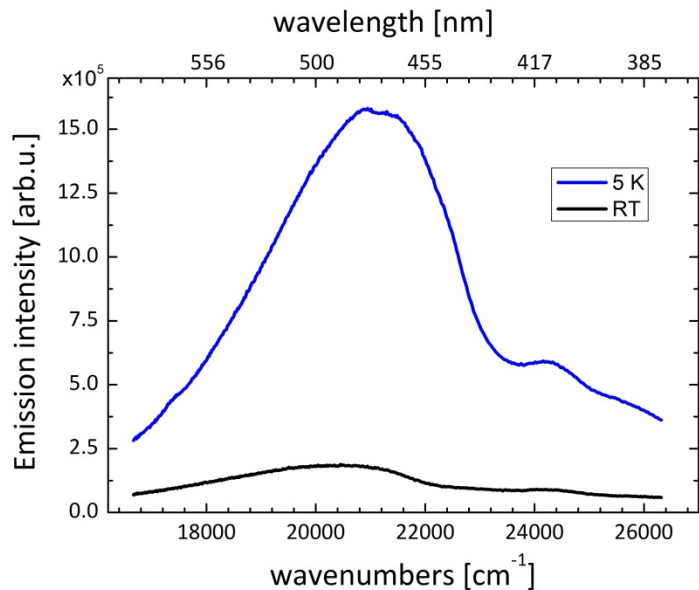


**Fig. S2.** Luminescence spectra of Dy<sub>3</sub> for room temperature (black line) and T = 5 K (blue line).

## MCD measurements:

MCD spectra were recorded with a home built spectrometer.

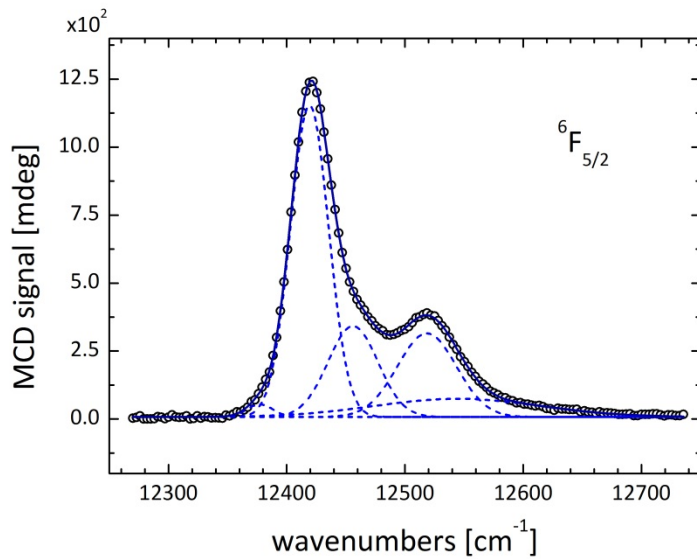


**Fig. S3.** MCD spectra of  $\text{Dy}_3$  showing the transition from the  $^6\text{H}_{15/2}$  to the  $^6\text{F}_{5/2}$  multiplet. The experimental spectrum is given by the black circles. Blue dashed lines represent single Gaussian fits and the solid dark blue line shows their sum.

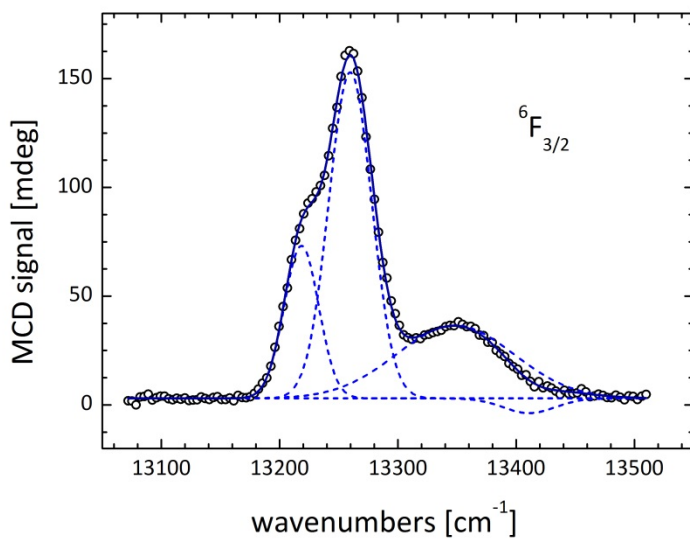


**Fig. S4.** MCD spectra of  $\text{Dy}_3$  showing the transition to the  $^6\text{F}_{3/2}$  multiplet. The experimental spectrum is given by the black circles. Blue dashed lines represent single Gaussian fits and the solid dark blue line shows their sum.

## Ab initio calculations

Mononuclear fragment calculations were done with MOLCAS 7.8 using the RASSCF/RASSI-SO/SINGLE\_ANISO routines. Basis sets were taken from the MOLCAS ANO-RCC library for dysprosium (Dy.ANO-RCC...8s7p5d4f2g1h). Complete active space self-consistent field (CASSCF) calculations include the Dy 4f orbitals (CAS(9 in 7)). Spin-orbit mixing within the restricted active space state interaction (RASSI-SO) procedure include all Sextets (<sup>6</sup>H, <sup>6</sup>F, and <sup>6</sup>P), 128 Quartet (<sup>4</sup>I, <sup>4</sup>F, <sup>4</sup>M, <sup>4</sup>G, <sup>4</sup>K, <sup>4</sup>L, <sup>4</sup>D, <sup>4</sup>H, <sup>4</sup>P, <sup>4</sup>G, <sup>4</sup>F and <sup>4</sup>I) and 130 Doublet terms (<sup>2</sup>L, <sup>2</sup>K, <sup>2</sup>P, <sup>2</sup>N, <sup>2</sup>F, <sup>2</sup>M, <sup>2</sup>H, <sup>2</sup>D, <sup>2</sup>G and <sup>2</sup>O). Second order multi configurational perturbation calculations (CASPT2) were not performed.

Table S1-S3 list the decomposition of the RASSSI wave functions corresponding to the lowest atomic multiplet J = 15/2 (squares of the coefficients) in the local coordinate frame of the corresponding Dy ion.

**Table S1.** Dy1 ( local coordinate system )

JM >	KD1-a	KD1-b	KD2-a	KD2-b	KD3-a	KD3-b	KD4-a	KD4-b
-15/2	0.00	0.98	0.00	0.00	0.00	0.00	0.00	0.00
-13/2	0.00	0.00	0.12	0.39	0.19	0.05	0.11	0.01
-11/2	0.00	0.01	0.02	0.09	0.02	0.03	0.17	0.09
-9/2	0.00	0.00	0.01	0.09	0.06	0.00	0.04	0.09
-7/2	0.00	0.00	0.01	0.02	0.01	0.06	0.18	0.07
-5/2	0.00	0.00	0.03	0.06	0.05	0.04	0.03	0.08
-3/2	0.00	0.00	0.04	0.03	0.02	0.20	0.02	0.02
-1/2	0.00	0.00	0.06	0.03	0.21	0.04	0.08	0.02
1/2	0.00	0.00	0.03	0.06	0.04	0.21	0.02	0.08
3/2	0.00	0.00	0.03	0.04	0.20	0.02	0.02	0.02
5/2	0.00	0.00	0.06	0.03	0.04	0.05	0.08	0.03
7/2	0.00	0.00	0.02	0.01	0.06	0.01	0.07	0.18
9/2	0.00	0.00	0.09	0.01	0.00	0.06	0.09	0.04
11/2	0.01	0.00	0.09	0.02	0.03	0.02	0.09	0.17
13/2	0.00	0.00	0.39	0.12	0.05	0.19	0.01	0.11
15/2	0.98	0.00	0.00	0.00	0.00	0.00	0.00	0.00
JM >	KD5-a	KD5-b	KD6-a	KD1-b	KD7-a	KD7-b	KD8-a	KD8-b
-15/2	0.00	0.01	0.00	0.00	0.00	0.01	0.00	0.00
-13/2	0.01	0.05	0.00	0.00	0.00	0.05	0.00	0.00
-11/2	0.06	0.21	0.01	0.09	0.01	0.16	0.01	0.01
-9/2	0.12	0.04	0.06	0.14	0.01	0.23	0.02	0.10
-7/2	0.02	0.09	0.01	0.15	0.01	0.15	0.03	0.18
-5/2	0.07	0.16	0.13	0.08	0.01	0.04	0.06	0.16
-3/2	0.05	0.10	0.10	0.09	0.04	0.08	0.10	0.11
-1/2	0.00	0.01	0.14	0.00	0.08	0.12	0.07	0.16
1/2	0.01	0.00	0.00	0.14	0.12	0.08	0.16	0.07
3/2	0.10	0.05	0.09	0.10	0.08	0.04	0.11	0.10
5/2	0.16	0.07	0.08	0.13	0.04	0.01	0.16	0.06
7/2	0.09	0.02	0.15	0.01	0.15	0.01	0.18	0.03
9/2	0.04	0.12	0.14	0.06	0.23	0.01	0.10	0.02
11/2	0.21	0.06	0.09	0.01	0.16	0.01	0.01	0.01
13/2	0.05	0.01	0.00	0.00	0.05	0.00	0.00	0.00
15/2	0.01	0.00	0.00	0.00	0.01	0.00	0.00	0.00

**Table S2.** Dy2 (local coordinate system )

JM >	KD1-a	KD1-b	KD2-a	KD2-b	KD3-a	KD3-b	KD4-a	KD4-b
-15/2	0.00	0.96	0.00	0.00	0.01	0.00	0.01	0.00
-13/2	0.00	0.00	0.00	0.74	0.13	0.00	0.00	0.00

-11/2	0.00	0.04	0.00	0.05	0.32	0.00	0.27	0.00
-9/2	0.00	0.00	0.00	0.18	0.04	0.00	0.07	0.00
-7/2	0.00	0.00	0.00	0.02	0.32	0.00	0.00	0.00
-5/2	0.00	0.00	0.00	0.00	0.13	0.01	0.25	0.00
-3/2	0.00	0.00	0.00	0.00	0.02	0.00	0.26	0.01
-1/2	0.00	0.00	0.00	0.00	0.01	0.00	0.08	0.04
1/2	0.00	0.00	0.00	0.00	0.00	0.01	0.04	0.08
3/2	0.00	0.00	0.00	0.00	0.00	0.02	0.01	0.26
5/2	0.00	0.00	0.00	0.00	0.01	0.13	0.00	0.25
7/2	0.00	0.00	0.02	0.00	0.00	0.32	0.00	0.00
9/2	0.00	0.00	0.18	0.00	0.00	0.04	0.00	0.07
11/2	0.04	0.00	0.05	0.00	0.00	0.32	0.00	0.27
13/2	0.00	0.00	0.74	0.00	0.00	0.13	0.00	0.00
15/2	0.96	0.00	0.00	0.00	0.00	0.01	0.00	0.01

JM >	KD5-a	KD5-b	KD6-a	KD1-b	KD7-a	KD7-b	KD8-a	KD8-b
-15/2	0.00	0.00	0.00	0.00	0.01	0.00	0.01	0.00
-13/2	0.00	0.02	0.01	0.00	0.00	0.05	0.01	0.04
-11/2	0.02	0.01	0.00	0.01	0.15	0.00	0.12	0.00
-9/2	0.01	0.17	0.07	0.00	0.01	0.23	0.03	0.18
-7/2	0.02	0.04	0.05	0.07	0.23	0.01	0.22	0.02
-5/2	0.00	0.11	0.13	0.00	0.02	0.16	0.04	0.15
-3/2	0.07	0.17	0.10	0.16	0.08	0.01	0.10	0.02
-1/2	0.26	0.10	0.29	0.12	0.00	0.02	0.02	0.06
1/2	0.10	0.26	0.12	0.29	0.02	0.00	0.06	0.02
3/2	0.17	0.07	0.16	0.10	0.01	0.08	0.02	0.10
5/2	0.11	0.00	0.00	0.13	0.16	0.02	0.15	0.04
7/2	0.04	0.02	0.07	0.05	0.01	0.23	0.02	0.22
9/2	0.17	0.01	0.00	0.07	0.23	0.01	0.18	0.03
11/2	0.01	0.02	0.01	0.00	0.00	0.15	0.00	0.12
13/2	0.02	0.00	0.00	0.01	0.05	0.00	0.04	0.01
15/2	0.00	0.00	0.00	0.00	0.00	0.01	0.00	0.01

**Table S3.** Dy3 ( local coordinate system )

JM >	KD1-a	KD1-b	KD2-a	KD2-b	KD3-a	KD3-b	KD4-a	KD4-b
-15/2	0.97	0.00	0.00	0.00	0.01	0.00	0.01	0.00
-13/2	0.00	0.00	0.00	0.85	0.06	0.00	0.00	0.00
-11/2	0.02	0.00	0.00	0.03	0.49	0.00	0.22	0.00
-9/2	0.00	0.00	0.00	0.11	0.09	0.00	0.16	0.03
-7/2	0.00	0.00	0.00	0.00	0.26	0.00	0.03	0.02
-5/2	0.00	0.00	0.00	0.00	0.05	0.01	0.28	0.01
-3/2	0.00	0.00	0.00	0.00	0.00	0.00	0.18	0.04
-1/2	0.00	0.00	0.00	0.00	0.00	0.01	0.01	0.02
1/2	0.00	0.00	0.00	0.00	0.01	0.00	0.02	0.01
3/2	0.00	0.00	0.00	0.00	0.00	0.00	0.04	0.18
5/2	0.00	0.00	0.00	0.00	0.01	0.05	0.01	0.28
7/2	0.00	0.00	0.00	0.00	0.00	0.26	0.02	0.03
9/2	0.00	0.00	0.11	0.00	0.00	0.09	0.03	0.16
11/2	0.00	0.02	0.03	0.00	0.00	0.49	0.00	0.22
13/2	0.00	0.00	0.85	0.00	0.00	0.06	0.00	0.00
15/2	0.00	0.97	0.00	0.00	0.00	0.01	0.00	0.01

JM >	KD5-a	KD5-b	KD6-a	KD1-b	KD7-a	KD7-b	KD8-a	KD8-b
-15/2	0.00	0.00	0.00	0.00	0.00	0.00	0.00	0.01
-13/2	0.01	0.00	0.01	0.01	0.00	0.01	0.00	0.05
-11/2	0.03	0.00	0.01	0.01	0.00	0.04	0.00	0.14
-9/2	0.14	0.03	0.02	0.09	0.01	0.08	0.00	0.23
-7/2	0.04	0.01	0.07	0.09	0.00	0.21	0.01	0.27
-5/2	0.04	0.03	0.08	0.00	0.02	0.28	0.01	0.18
-3/2	0.10	0.07	0.28	0.03	0.06	0.16	0.00	0.08
-1/2	0.21	0.29	0.30	0.01	0.03	0.10	0.00	0.02
1/2	0.29	0.21	0.01	0.30	0.10	0.03	0.02	0.00
3/2	0.07	0.10	0.03	0.28	0.16	0.06	0.08	0.00
5/2	0.03	0.04	0.00	0.08	0.28	0.02	0.18	0.01

7/2	0.01	0.04	0.09	0.07	0.21	0.00	0.27	0.01
9/2	0.03	0.14	0.09	0.02	0.08	0.01	0.23	0.00
11/2	0.00	0.03	0.01	0.01	0.04	0.00	0.14	0.00
13/2	0.00	0.01	0.01	0.01	0.01	0.00	0.05	0.00
15/2	0.00	0.00	0.00	0.00	0.00	0.00	0.01	0.00

### Description of the exchange interaction

Hamiltonian:

$$\mathcal{H} = -j_{12}\hat{\tilde{S}}_1 \cdot \hat{\tilde{S}}_2 - j_{13}\hat{\tilde{S}}_1 \cdot \hat{\tilde{S}}_3 - j_{23}\hat{\tilde{S}}_2 \cdot \hat{\tilde{S}}_3$$

$j_{ij}$  is the total magnetic interaction: exchange + dipolar;

$s_{ij}$  are local pseudospins ( $s=1/2$ ) on Dy sites ( i.e. the lowest Kramers doublet)

The dipolar interaction is treated exactly ( entirely ab initio).

The exchange interaction is fitted to the available experiment.

**Table S4.** Decomposition of magnetic couplings (values in  $\text{cm}^{-1}$ )

Interaction	Dipolar	Exchange	Total
1 - 2	4.491	2.960	7.451
1 - 3	4.524	2.821	7.345
2 - 3	4.408	3.284	7.692

## EPR investigations

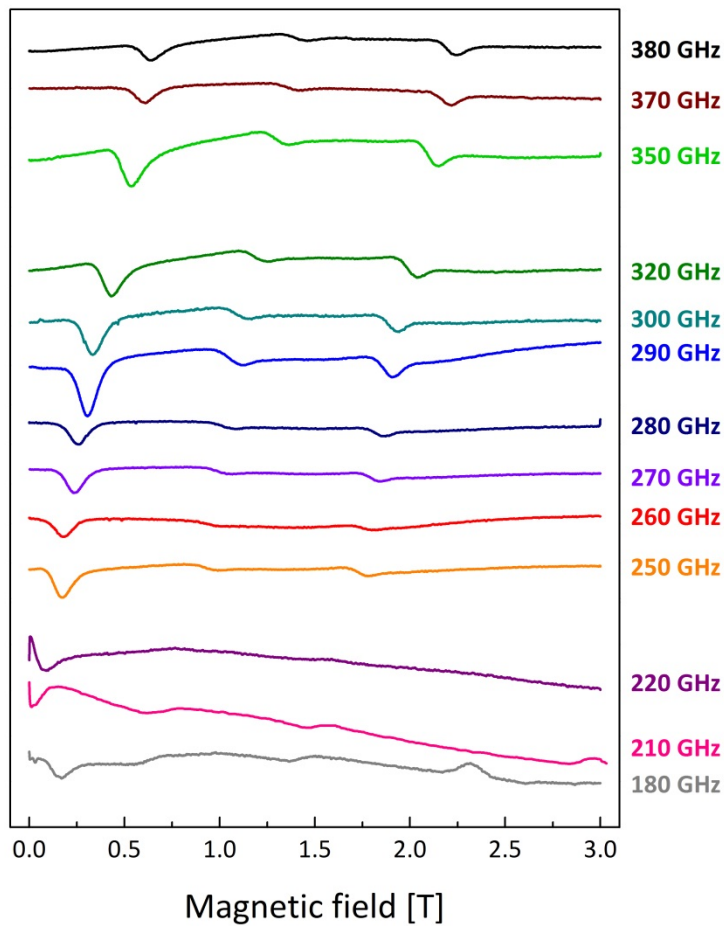


**Fig. S5.** Experimental EPR data at 4.2 K for all applied microwave frequencies as indicated.

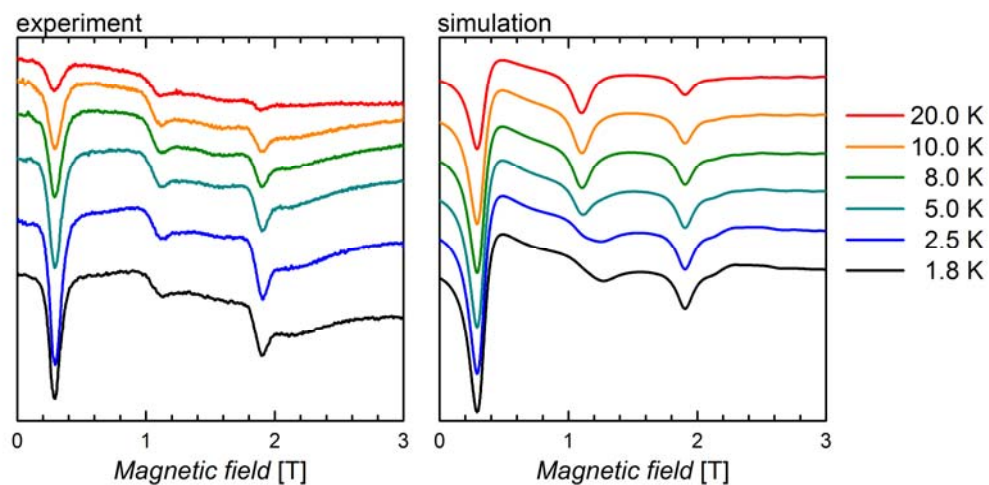


**Fig. S6.** Experimental (left) and simulated (right) EPR data for a microwave frequency of 290 GHz at different temperatures as indicated. Simulations were carried out using the pseudo spin  $\frac{1}{2}$  model with the best fit parameters (see main text).

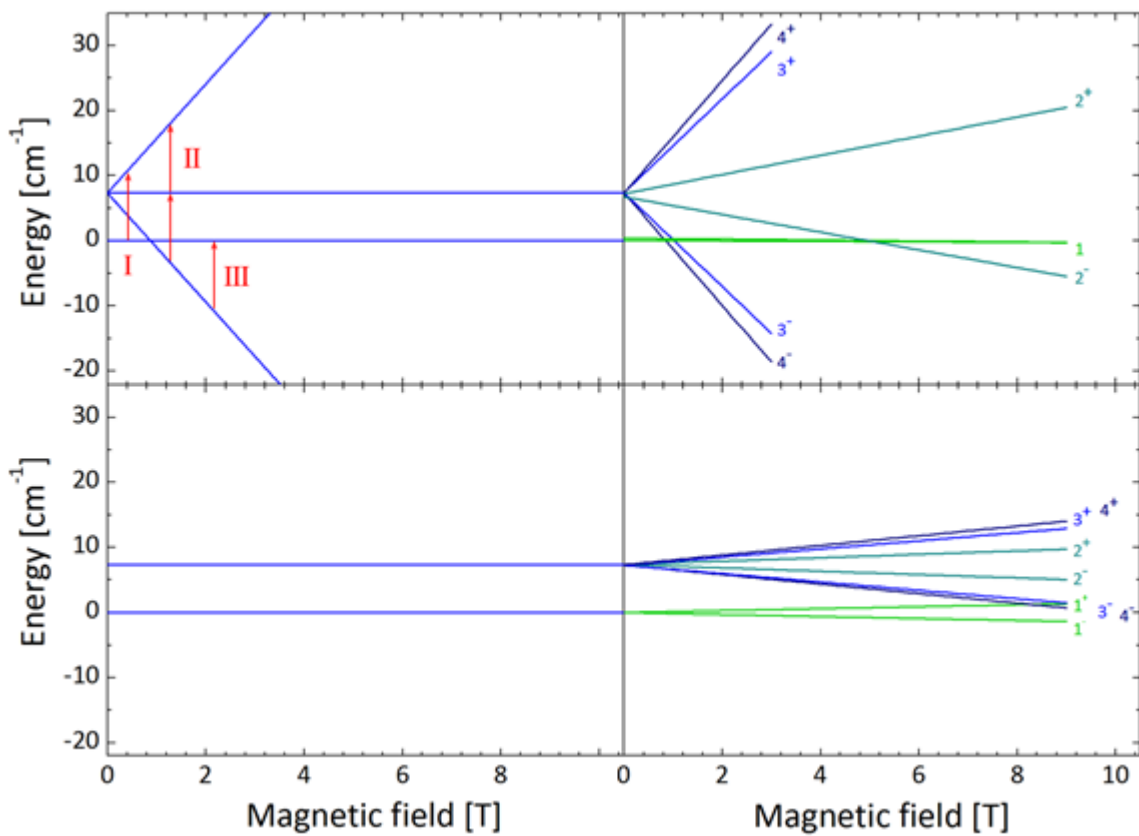


**Fig. S7.** Energy level diagram calculated for an effective spin  $\frac{1}{2}$  model for an idealized trigonal symmetry (left) and considering the real angles of the easy axes of the single Dy ions (right) for a magnetic field applied in the triangle plane (top) and perpendicular to it (bottom). The corresponding wave functions ( $1^{\pm}-4^{\pm}$ ) can be found in Ref<sup>1</sup>.

## FIR investigations

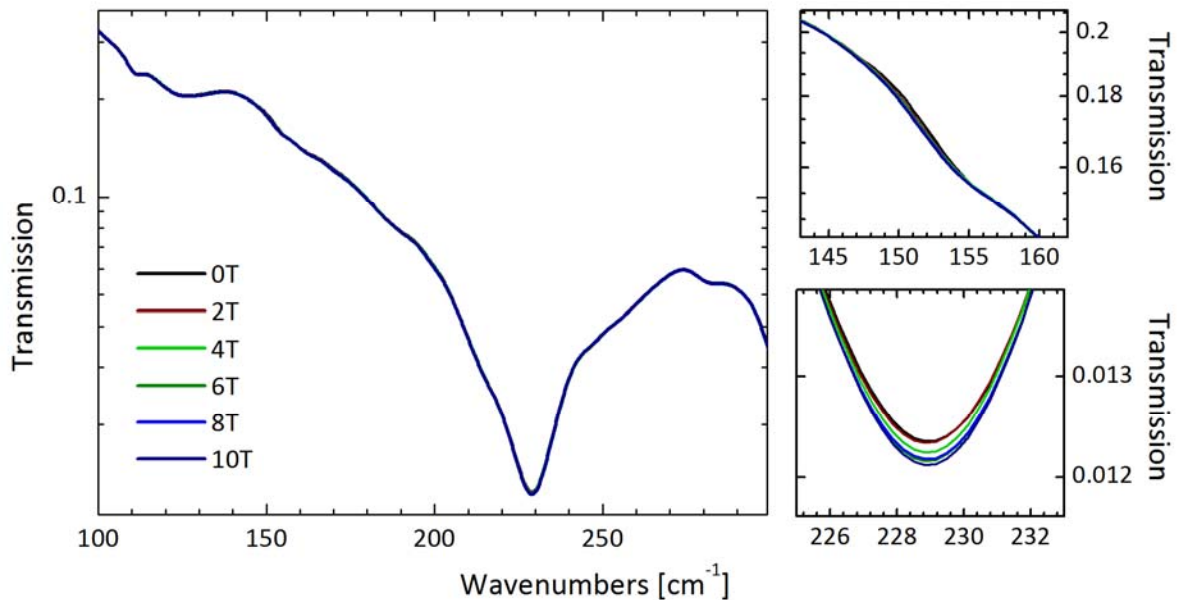


**Fig. S8.** FIR transmission spectra of the  $\text{Dy}_3$  triangle at 4.2K. Right: Blow-ups of the relevant regions.

## Torque investigations

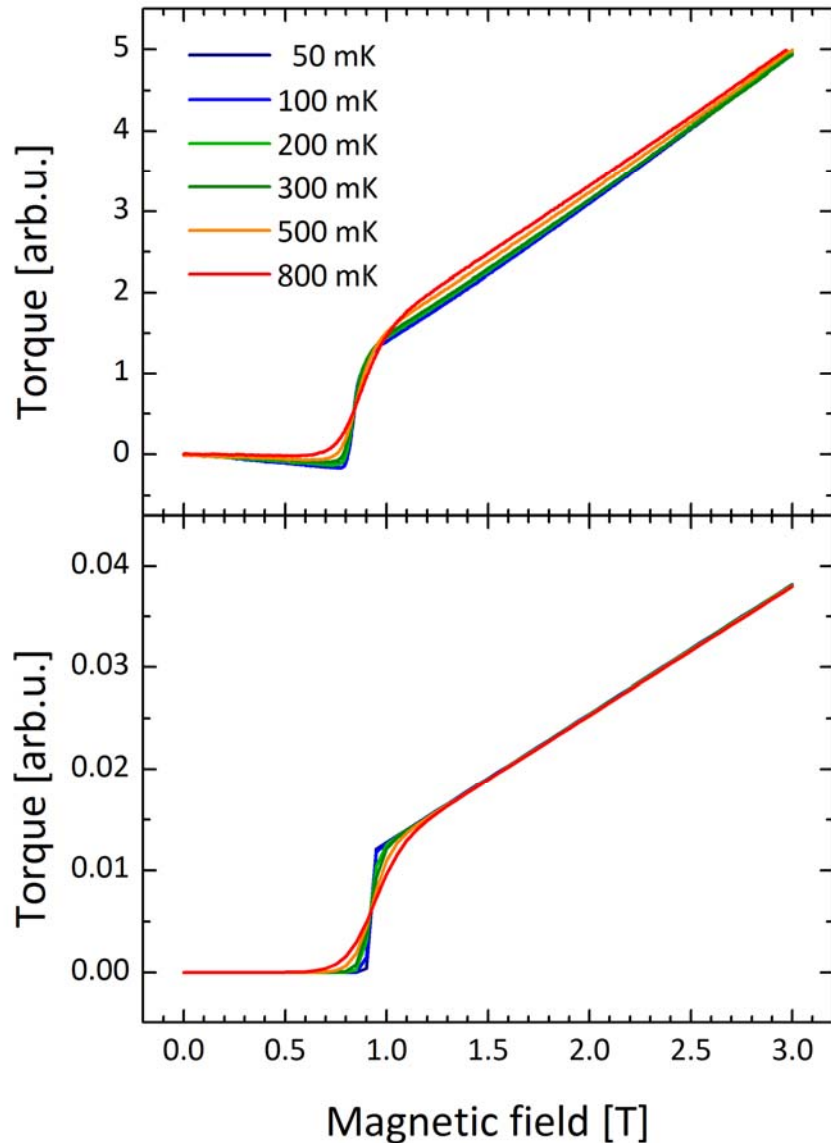


**Fig. S9.** Top: Temperature dependence of the averaged torque signals in the triangle plane for  $\alpha=5.2^\circ$ . Bottom: Simulated averaged torque curves of the Dy<sub>3</sub> triangle for the best fitting parameters derived from FIR and torque measurements (see main text).

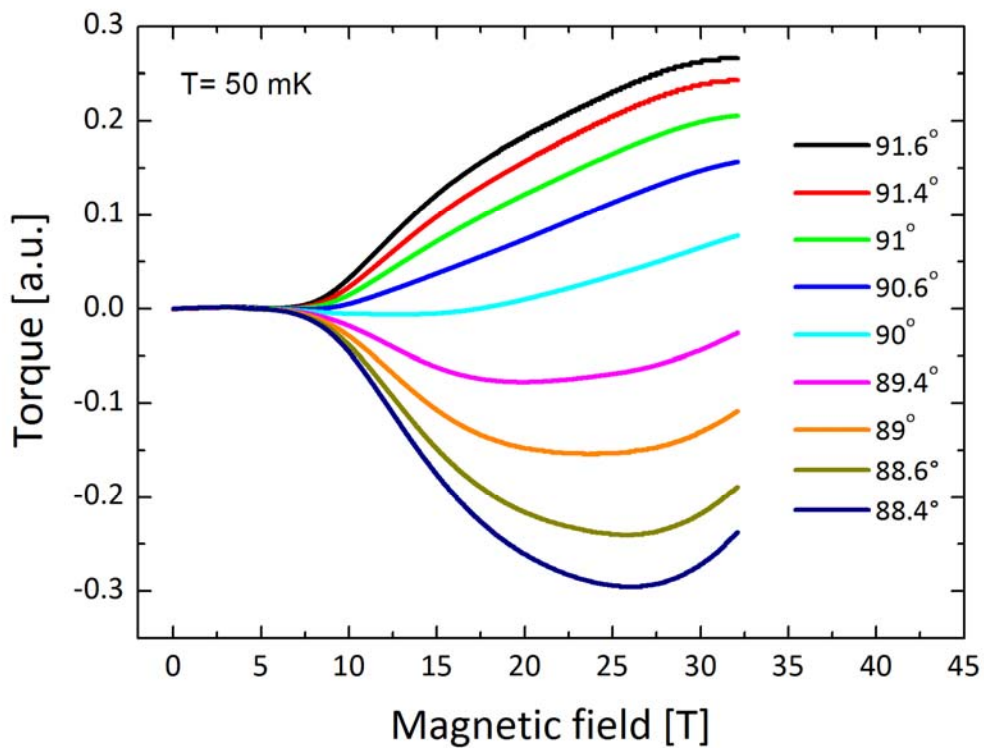


**Fig. S10.** Raw experimental torque data for angles close to  $90^\circ$  at 0.05 K.

## Improvement of the model

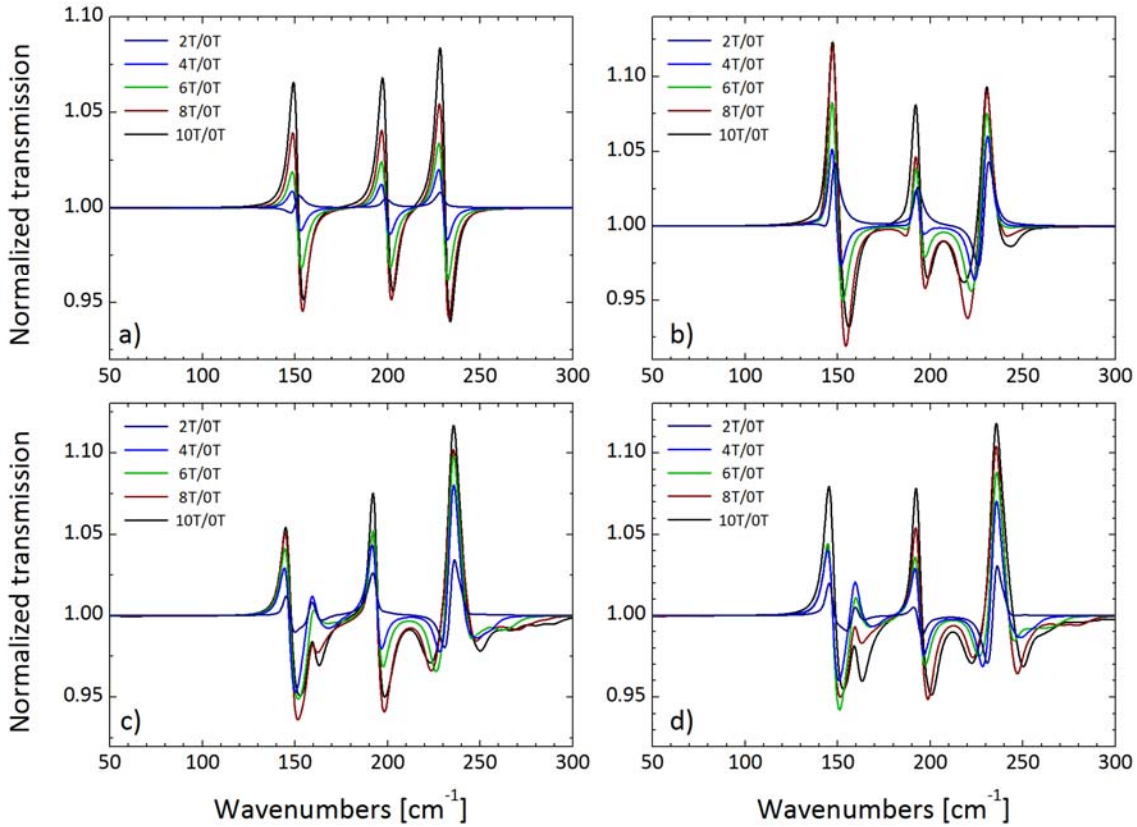


**Fig. S11.** Influence of the wave functions of the single dysprosium ions on the FIR spectra. (a) Simulated FIR spectra for diagonal matrix elements  $\delta_1 = 150$ ,  $\delta_2 = 229$ ,  $\delta_3 = 198$  cm<sup>-1</sup>. Furthermore, an idealized trigonal symmetry (easy axes related by 120° rotations) and pure ground and excited states are assumed. (b) Calculated FIR spectra incorporating only diagonal matrix elements  $\delta_1 = 229$ ,  $\delta_2 = 147$ ,  $\delta_3 = 192$  cm<sup>-1</sup>, and assuming idealized orientations of the local anisotropy axes. The wave functions of the ground and first excited state of each dysprosium ion are given by ab initio results (Table S1-S3). (c) Simulated FIR spectra assuming a perfect trigonal symmetry of the local anisotropy axes and additionally incorporating off-diagonal matrix elements with the best fitting parameters described in the main text. (d) Simulated FIR spectra as for (c) assuming a different orientation of the single ion easy axes. The angles in and out of the triangle plane are given by ab initio calculations.

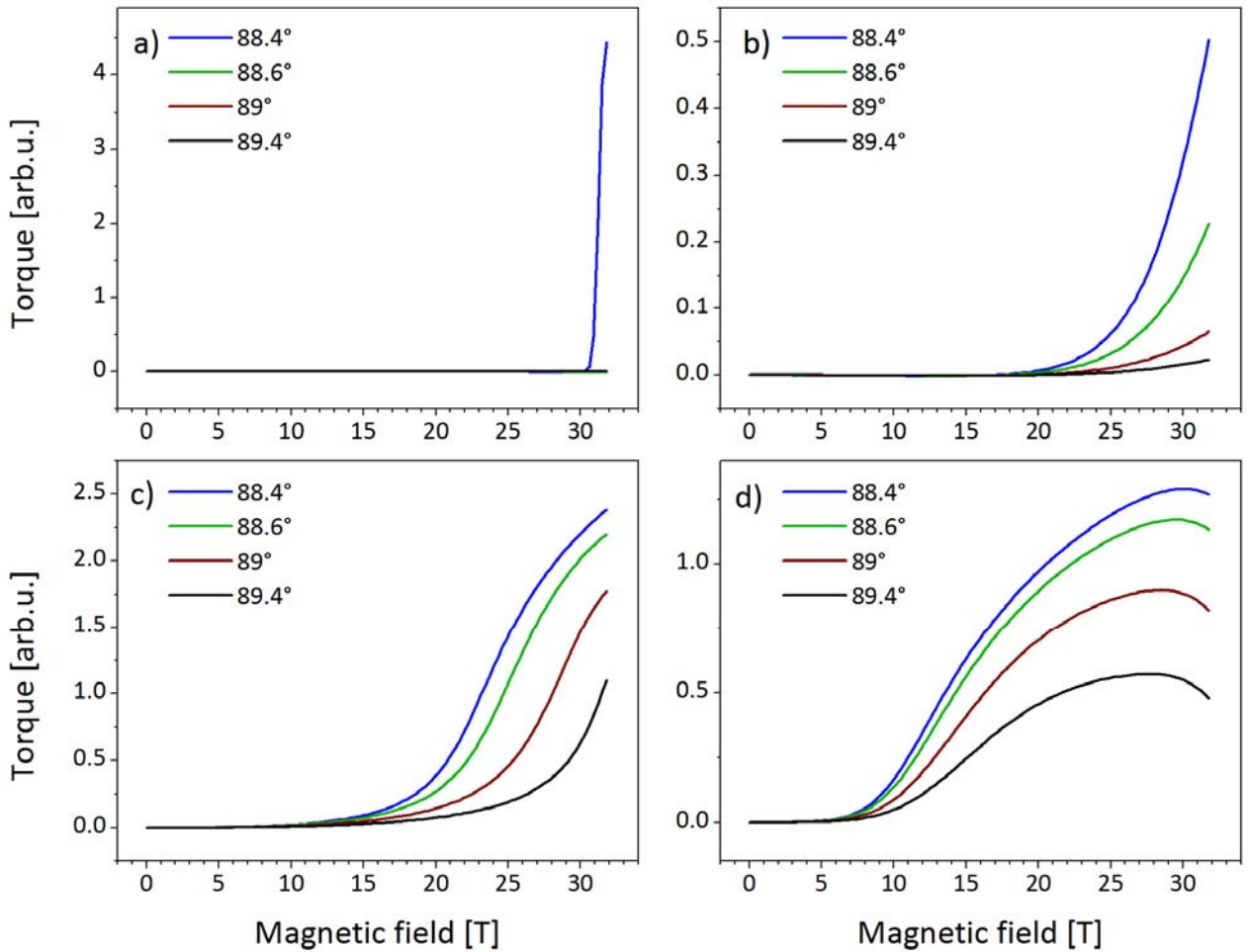


**Fig. S12.** Influence of the wave functions of the single dysprosium ions on the torque signals. (a) Simulated torque signals for diagonal matrix elements only ( $\delta_1 = 150$ ,  $\delta_2 = 229$ ,  $\delta_3 = 198 \text{ cm}^{-1}$ ). Furthermore an idealized trigonal symmetry (easy axes related by  $120^\circ$  rotations) and pure ground and excited states are assumed. (b) Calculated torque signals incorporating only diagonal matrix elements  $\delta_1 = 229$ ,  $\delta_2 = 147$ ,  $\delta_3 = 192 \text{ cm}^{-1}$ , and assuming idealized orientations of the local anisotropy axes. The wave functions of the ground and first excited state of each dysprosium ion are given by ab initio results (Table S1-S3). (c) Simulated torque signals assuming a perfect trigonal symmetry of the local anisotropy axes and additionally incorporating off-diagonal matrix elements with the best fitting parameters described in the main text. (d) Same torque simulations including of diagonal matrix elements as given in (c) with different orientation of the single ion easy axes. The angles in and out of the triangle plane are given by ab initio calculations.

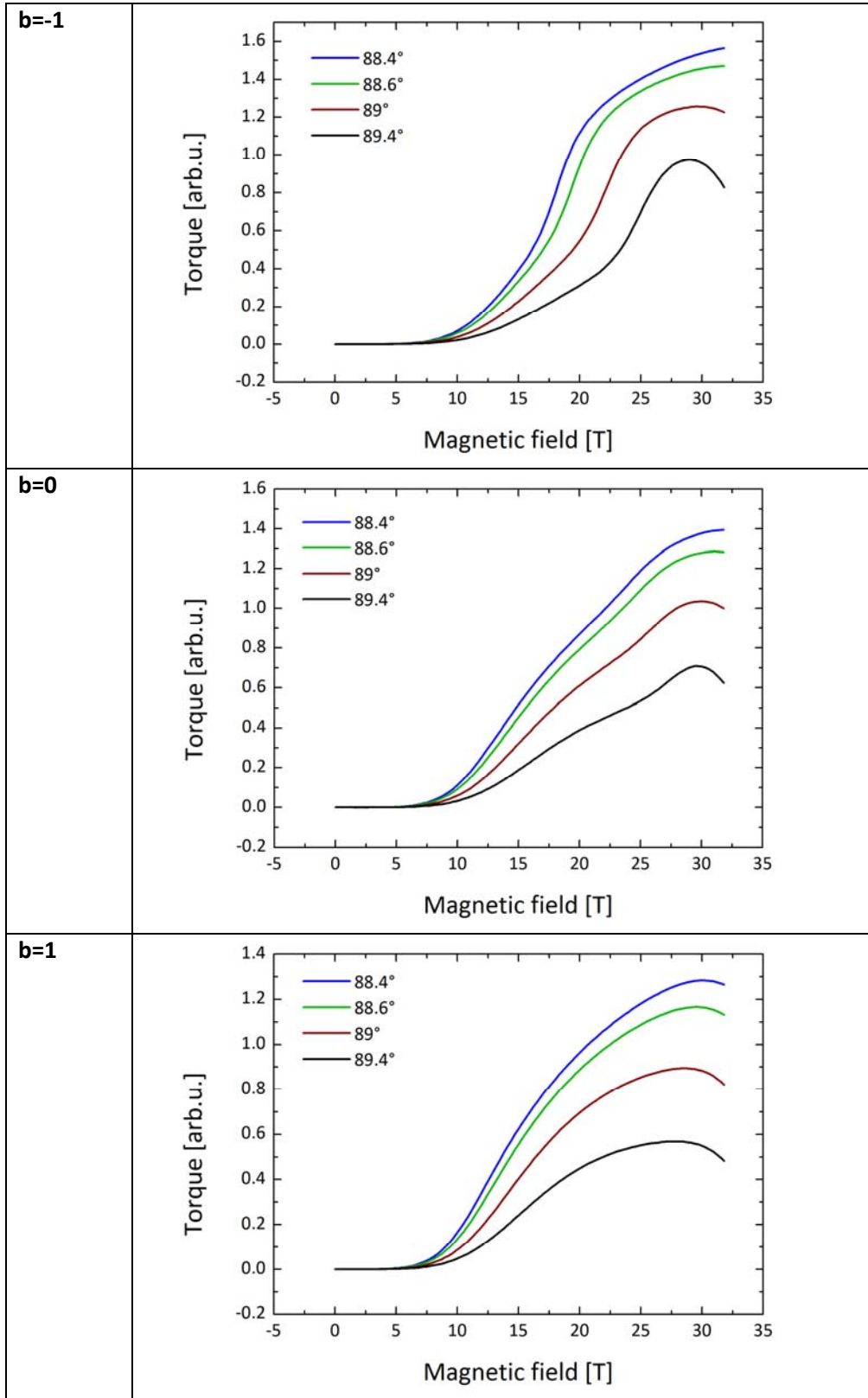


**Fig. S13.** Influence of the alignment of the easy axes of the single dysprosium ions in the triangle plane on the calculated torque signal given by the parameter  $b$ :  $\varphi_i = b \cdot \varphi_{i,ab initio}$ . Calculations were performed for the best fit parameter  $a = 0.9$  (with  $\theta_i = a \cdot \theta_{i,ab initio}$ , angle out of the triangle plane) and the best off-diagonal matrix elements of the single ion zero-field matrices  $\delta_1 = 229$ ,  $\delta_2 = 147$ ,  $\delta_3 = 192$ ,  $ge_1' = -8$ ,  $ge_2 = 4$ ,  $ge_3 = 1$ ,  $ee_2 = 2 \text{ cm}^{-1}$ .

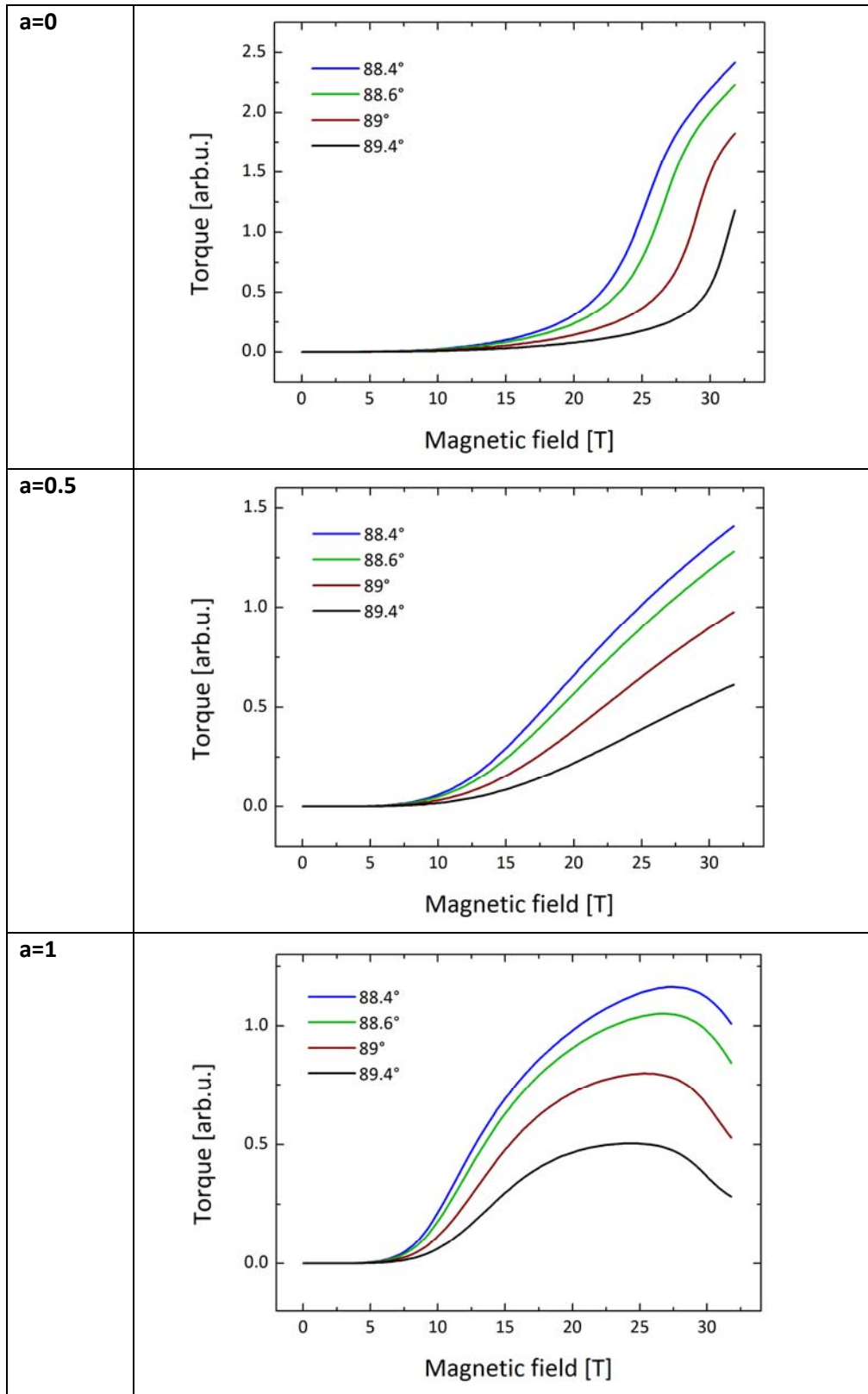


**Fig. S14.** Influence of the alignment of the easy axes of the single dysprosium ions perpendicular to the triangle plane on the calculated torque signal given by the parameter  $a$ :  $\theta_i = a \cdot \theta_{i,ab initio}$ . Calculations were performed for the best fit parameter  $b = 1$  (with  $\varphi_i = b \cdot \varphi_{i,ab initio}$ , angle in the triangle plane) and the best off-diagonal matrix elements of the single ion zero-field matrices  $\delta_1 = 229$ ,  $\delta_2 = 147$ ,  $\delta_3 = 192$ ,  $ge_1' = -8$ ,  $ge_2 = 4$ ,  $ge_3 = 1$ ,  $ee_2 = 2 \text{ cm}^{-1}$ .

## **Supplementary references**

1. L. Ungur, W. Van den Heuvel and L. F. Chibotaru, *New J. Chem.*, 2009, 33, 1224-1230.